Article

Mannosylated Polyion Complexes for In Vivo Gene Delivery into CD11c+ Dendritic Cells

Lior Raviv, Michal Jaron-Mendelson, and Ayelet David

Mol. Pharmaceutics, **Just Accepted Manuscript** • DOI: 10.1021/mp5005492 • Publication Date (Web): 22 Dec 2014

Mannosylated Polyion Complexes for *In Vivo* Gene Delivery into CD11c$^+$ Dendritic Cells

Lior Raviv[a], Michal Jaron-Mendelson[b], and Ayelet David[a,*]

[a] Department of Clinical Biochemistry and Pharmacology, Faculty of Health Sciences, and Ilse Katz Institute for Nanoscale Science and Technology, Ben-Gurion University of the Negev, Beer-Sheva, 84105, Israel

[b] Shraga Segal Department of Microbiology and Immunology, Faculty of Health Sciences, Ben-Gurion University of the Negev, Beer-Sheva 84105, Israel

*** Corresponding Author**

Department of Clinical Biochemistry and Pharmacology

Faculty of Health Sciences, Ben-Gurion University of the Negev

Beer-Sheva 84105, Israel

Tel: +972-8-6477364; Fax: +972-8-6479303

E-mail: ayeletda@bgu.ac.il

Running title: Mannosylated polyion complexes for targeting dendritic cells

Keywords: Dendritic cells, gene delivery system, mannose receptor, mannose-receptor ligands, multivalency

ABSTRACT

Dendritic cells (DCs) possess unique abilities in initiating primary immune responses and thus represent prime targets for DNA-based vaccinations. Here, we describe the design and synthesis of mannosylated polyion complexes (PICs) composed of cationic polyethylenimine (PEI) and hydrophilic polyethylene glycol (PEG) segments, and bearing mono- and tri-valent mannose as ligand for targeting mannose receptor (MR/CD206)-positive DCs. Amino-terminated mannose (Man)-containing ligands in mono- and tri-valent presentations (Man- and Man_3-, respectively) were prepared and conjugated to PEG via an N-hydroxysuccinimide (NHS)-activated terminal. Thiolated PEI was conjugated to the mannosylated PEG via the maleimide (MAL)-activated terminal. The resulting positively charged di-block copolymers bearing mannoses (Man-PEG-*b*-PEI and Man_3-PEG-*b*-PEI) were self-assembled with DNA to form PICs with lower surface charge than did their PEI building block and mean hydrodynamic diameters in the range of 100-450 nm, depending on the N/P ratio. Man_3-PEG-*b*-PEI demonstrated a 3-4-fold greater transfection efficiency in MR-positive dendritic cell lines (THP-1, DC2.4), relative to Man-PEG-*b*-PEI, exhibited low cytotoxicity when compared with PEI and showed low transfection efficiency in non-dendritic HeLa cells. In preliminary *in vivo* experiments, Man-PEG-*b*-PEI/DNA and Man_3-PEG-*b*-PEI/DNA demonstrated 2-3-fold higher gene delivery efficiency into CD11c+ DCs collected from inguinal lymph nodes of C57/BL6 mice, when compared to PEI/DNA complexes, as shown by GFP expression measurements, 24 h post subcutaneous injection. The results indicate that the mannosylated PICs are safe and effective gene delivery system, showing *in vivo* specificity towards CD11c+ DCs that over-express the MR.

ABBREVIATIONS

APCs	antigen-presenting cells
CRDs	carbohydrate recognition domains
DMSO	dimethyl sulfoxide
EtBr	ethidium bromide
MAL	maleimide
Man	mannose
MR	mannose receptor
MHC	major histocompatibility complex
MTT	3-(4,5-dimethylthiazol-2-yl)-2,5-diphenyltetrazolinium bromide
NHS	N-hydroxysuccinimide
PBS	phosphate-buffered saline
PEG	polyethylene glycol
PEI	polyethylenimine
SATA	N-succinimidyl-S-acetylthioacetate
TEA	triethylamine

INTRODUCTION

Dendritic cells (DCs) are the most potent professional antigen-presenting cells known [1]. Their ability to capture, process, and present foreign antigens, migrate to lymphoid-rich tissues, and stimulate cellular antigen-specific immune responses makes them an ideal tool for cancer immunotherapy. Genetic approaches to antigen loading, based on physical, viral- and non-viral-based transfer of vaccine DNA into DCs, offers the advantage of a continuous supply of antigen for presentation of vaccine antigens on MHC class I and II products [2]. To date, adenovirus vectors have been found to be the most efficient gene delivery system for DCs. However, adenoviruses are highly immunogenic and can elicit potent anti-viral immune responses that restrict their application in medical therapy. Accordingly, different types of non-viral delivery vehicles have been developed for gene delivery, with lipid- or polymer-based complexes (lipoplexes or polyplexes, respectively) currently being the most commonly employed [3]. Polyplexes consist a cationic segment as a core component that can self-assemble through electrostatic interactions with oligonucleotides to produce polyion complexes (PICs), within which DNA is encapsulated [4-6]. Polyethylenimine (PEI) is one of the most useful polycations for DNA binding and condensation as it demonstrates high transfection efficiency and pH buffering capacity, which is believed to protect DNA from degradation and to enable its escape from the endosomal compartment [7, 8]. However, the positive surface charge of PEI/DNA polyplexes results in aggregation, adsorption to plasma proteins, non-specific interaction with cells, recognition by immune system components, and cytotoxicity [9-11]. Modification of PEI by polyethylene glycol (PEG) can increase polymer solubility, protect PICs from macrophage uptake, prolong circulation time *in vivo*, and decrease non-specific interactions with serum protein [12-15.] Yet, PEG-PEI/DNA complexes can show reduced cellular uptake as

compared to positively charged PICs due to reduced interactions with the negatively charged cellular membrane. Together with the fact that DCs compose only 1-3% of cells in peripheral tissues [16-19], the system may have a very limited efficiency unless targeted. The attachment of cell-specific ligand to the PEG-PEI/DNA complex surface is expected to improve transfection efficiency and enhance cellular uptake via receptor-mediated endocytosis.

Mannose receptor (MR/CD206) is a 175 kDa transmembrane protein highly expressed on DCs and macrophages and up-regulated in tumor-associated macrophages [20]. It contains eight C-type carbohydrate recognition domains (CRDs) per polypeptide [21, 22] and mediates the endocytosis and processing of antigens that expose mannose and fucose residues for presentation by major histocompatibility complex (MHC) class II molecules [23]. It has been previously demonstrated that mannosylated lipoplexes and polyplexes can be used for gene delivery into macrophages and DCs [24-32]. The eight adjacent CRDs in MR may further help to increase the binding affinity and specificity of lipoplexes and polyplexes containing, D-mannose- and L-fucose-containing glycans in a multivalent display. Several research groups have synthesized multivalent mannosylated ligands and demonstrated higher *in vitro* binding affinity for the MR than the mono-mannosylated analogs [33, 34]. However, the influence of mannose valency on the targeting of DCs *in vivo* has not been tested yet.

In this study we synthesized mannosylated polyion complexes (PICs) composed of cationic linear PEI (25 kDa) and hydrophilic PEG (3.5 kDa) segment, and bearing mono- and tri-valent mannoses for actively targeting MR-positive DCs through multivalent interactions. We, moreover, evaluate their targeting ability and activity both *in vitro* and *in vivo.* We found that the PICs bearing manosylated ligands in tri-valent presentation (Man_3) demonstrated higher gene delivery efficiency into CD11c+ cells

collected from inguinal lymph nodes, when compared to mono-mannosylated PIC or non-mannosylated PICs. To the best of our knowledge, this is the first study to evaluate Man_3-PEG-*b*-PEI copolymer for gene delivery applications and it is the first attempt to evaluate the effect of the Man valency on PEG-*b*-PEI/DNA complexes on gene expression efficiency *in vivo*.

EXPERIMENTAL SECTION

Materials

All chemicals were of reagent grade and obtained from Sigma–Aldrich (Rehovot, Israel), unless otherwise noted. Linear PEI "Max" Mw 40,000 (Equivalent to Mw 25,000 Da in Free Base Form) was purchased from Polysciences Inc. (Eppenheim, Germany). N-succinimide-PEG-maleimide ester (NHS-PEG-MAL; MW 3,500 Da) was purchased from JenKem Technology USA Inc. (Allen, TX). The plasmid DNA encoding firefly luciferase and GFP (pCMVLuc and pGFP) were a gift from Prof. Moshe Oren (Weizmann Institute of Science, Rehovot, Israel). Dialysis tubing with 12,000-14,000 g/mol Mw cut-off was purchased from Cellu Sep T4, Membrane Filtration Products, Inc. (Segiun, TX, USA).

Cell lines and culture media

THP-1 monocytic leukemia cells were cultured in RPMI-1640 medium supplemented with 10% fetal bovine serum, 2 mM L-glutamine, 100 units/ml penicillin and 100 μg/ml of streptomycin. For differentiation to immature DCs, the following cytokine cocktail was added to the THP-1 cells medium: rhIL-4 (100 ng/ml = 1500 units/ml), rhGM-CSF (100 ng/ml = 1500 units/ml) [35]. DC2.4 cells were cultured in RPMI-1640 medium supplemented with 10% fetal bovine serum, 2 mM L-glutamine, 20 units/ml penicillin

and 20 μg/ml of streptomycin supplemented with 50 μM 2-mercaptoethanol. HeLa cells were cultured in DMEM supplemented with 10% fetal bovine serum, 2 mM L-glutamine, 100 units/ml penicillin and 100 μg/ml of streptomycin. Cells were grown at 37°C in a humidified atmosphere of 5% (v/v) CO_2 in air.

Synthesis of a monovalent Man targeting moiety, 4-aminophenyl α-D-mannopyranoside (Man-PAP)

4-nitrophenyl α-D-mannopyranoside (Man-PNP) was reduced to 4-aminophenyl α-D-mannopyranoside **(**Man-PAP) in methanol (MeOH) with ammonium formate (NH_4HCO_2) and in the presence of 10% palladium on carbon (Pd/C), as described [36]. Briefly, PNP-Man (151 mg, 0.2 mmol), NH_4HCO_2 (250 mg, 4 mmol) and Pd/C (25 mg) were dissolved in 30 ml MeOH. The mixture was gently warmed to 50°C while stirring to afford PAP-Man. The reaction mixture was then filtered, the solvent was evaporated, the product was dissolved in double distilled water and purified on PD-10 desalting column. PAP-Man was identified by thin layer chromatography (TLC).

Synthesis of trivalent-Man targeting moiety, Man_3-(amidohexanamido)-Tris (Man_3-AHT)

Man_3-AHT was synthesized based on a previously described procedure [36]. Briefly, Tris (0.97 g, 8 mmol) was first coupled with Cbz-aminohexanoic acid (2.4 g, 9 mmol) in absolute ethanol (500 ml) in the presence of 2-ethoxy-*N*-(ethoxycarbonyl)-1,2-dihydroquinoline (EEDQ) (2.66 g, 10.8 mmol) to afford (6-(benzyloxycarbonamido)hexanamido)-tris(hydroxymethyl)methane (Cbz-AHT) (Fig. 1A). α-D-Man (180 mg, 1 mmol) was transformed into 2,3,4,6-tetra-O-acetyl-α-D-mannopyranosyl bromide using 45% (w/v) HBr in glacial acetic acid (1 ml) (Fig. 1B),

and then coupled with [6-(benzyloxycarbonamido)hexanamido]-tris(hydroxymethyl)methane (Cbz-AHT) (0.5 mmol) in 10 ml mixture of nitromethane:toluene (1:1 (v/v)) in the presence of mercuric cyanide (0.5 mmol) to give the [6-(benzyloxycarbonamido)hexanamido]-tris(2,3,4,6-tetra-*O*-acetyl-α-D-mannopyranosyloxymethyl)methane (Cbz-AHT-[Man$(OAc)_4]_3$) conjugate (Fig. 1C). Cbz-AHT-[Man$(OAc)_4]_3$ (0.2 mmol)was purified on Sephadex LH-20 resin and de-acetylated in dry methanol containing 0.5 M sodium methoxide ($NaOCH_3$, 7.5 mmol) to give Cbz-AHT-$[Man]_3$. The Cbz protecting group was removed by hydrogenation in methanol using 10% Pd/C in the presence of ammonium formate (NH_4HCO_2) to give the desired Man_3-AHT. H^1-NMR and matrix-assisted laser desorption/ionization time of flight (MALDI-TOF) analysis were performed after each synthesis step to confirm the structure of Man_3-AHT and intermediate products (Fig. 1s, in Supplemental data),

Synthesis of mannosylated PEG-MAL

Man_3-AHT or Man-PAP was conjugated to NHS-PEG-MAL via the NHS-activated terminal in dimethyl sulfoxide (DMSO) to give Man_3-PEG-MAL or Man-PEG-MAL (Fig. 2A). Briefly, NHS-PEG-MAL (0.013 mmol) was dissolved in DMSO (400 µl). AHT-Man_3 or PAP-Man (0.13 mmol) were dissolved in DMSO (500 µl) in the presence of TEA (0.13 mmol) and then added to PEG solution. The reaction was carried out for 3 h at room temperature with shaking. Man-PEG-MAL or Man_3-PEG-MAL were precipitated in ether, isolated and characterized by ^{1}H-NMR.

Synthesis of mannosylated PEG-*b*-PEI, Man_3-PEG-*b*-PEI or Man-PEG-*b*-PEI

A thioacetate group was introduced into PEI (25000 Da) (0.004 mmol) by activation with N-succinimidyl-S-acetyl thioacetate (SATA) (0.024 mmol) in 5 ml DMSO in the

presence of triethylamine (TEA) and converted into a free sulphydryl group by subsequent treatment with 0.5 M hydroxylamine (NH_2OH) in PBS containing EDTA disodium (25mM), according to the manufacturer's protocol (Fig. 2B). Thiolated PEI (PEI-NH-CO-CH_2-SH) (0.001 mmol) was then conjugated to the mannosylated PEG (0.01 mmol) via the MAL-activated terminal in 3 ml PBS (pH 6.5) (Fig. 2C), based on a previously described procedure [37]. Man_3-PEG-*b*-PEI or Man-PEG-*b*-PEI were dialyzed (12,000-14,000 Da cut-off), lyophilized and characterized by ^{1}H-NMR and phenol/sulfuric acid assay [38]. PEG-*b*-PEI block-copolymers were synthesized as a control in a similar manner.

Complexation of mannosylated blocks copolymer with DNA and characterization

Block-copolymers and DNA (pCMVLuc or pGFP, 50 μg)) were separately dissolved in50 μl of 150mM NaCl. Following the addition of block-copolymer solution into the DNA solution, the mixture was vortexed for 15 seconds, spun down and incubated for 20 min at room temperature for complexation. Mean hydrodynamic size of the complexes was characterized by dynamic light scattering (DLS, CGS-3 LSE-5004, ALV-Laser Vertriebsgesellschaft m-b.H., Langen, Germany) at a scattering angle of 90° through a 400 μm pinhole at room temperature, and Surface charge was determined by ζ-potential measurements (Zetasizer Nano ZS, Malvern Instruments Ltd, Worcestershire, UK) in 150mM NaCl. Average values of the ζ-potential were calculated with the data from 9 measurements.

Ideal N/P ratio determination

Ideal N/P ratio for complexation (the ratio of amine groups on the block-copolymer to phosphate groups on the DNA) was determined Ethidium bromide (EtBr) exclusion

assay [39]. Briefly, triplicates of pGFP (4.3 µg) were complexed with increasing amounts of PEI, PEG-*b*-PEI, Man-PEG-*b*-PEI or Man_3-PEG-*b*-PEI (N/P: 0, 4, 8, 12) in 96-well dark, as described above. After 20 min incubation**,** 20 µl EtBr solution (0.1 mg/ml) were added. Fluorescence was measured on a Plate Luminol Luminescence Analyzer at λ_{ex}=518 nm and λ_{em}=605 nm. Results are given as relative fluorescence, with the fluorescence of DNA alone (N/P=0) with ethidium bromide considered as 100%.

Transfection efficacy *in vitro*

THP-1 or DC2.4 cells were plated in 12-well plates (1.5×10^5 cells/well) and grown 24 h before transfection. 2.8 µg of pCMVLuc or pGFP (8.5 nmol) were used to prepare PEI/DNA, PEG-*b*-PEI/DNA, Man-PEG-*b*-PEI/DNA and Man_3-PEG-*b*-PEI/DNA complexes at N/P=8, as described above, and the resulting Man_3-PEG-*b*-PEI/pCMVLuc and Man-PEG-*b*-PEI/pCMVLuc complexes were used to transfect the cells in 10% serum containing medium. PEI/pCMVLuc and PEG-*b*-PEI/pCMVLuc controls were tested likewise. Following 24h incubation with complexes, cells were washed twice with PBS and lysed by 15 minutes incubation with Cell Culture Lysis Buffer (Promega), with shaking. Luciferase gene expression was then monitored using the Luciferase 1000 Assay System (Promega), and Relative luminescent Units (RLU) were measured by a microplate reader (Infinite M200, TECAN, Switzerland). Protein content in the cells was determined by Bradford assay using the Protein Assay Dye Reagent (Bio-Rad) to normalize gene expression measurements. Normalized transfection efficiency values are presented as RLU/mg protein. GFP expression was monitored to quantify pGFP transfection efficiency. Transfected cells were visualized by fluorescence microscopy, and analyzed by flow-cytometry (Guava Easy Cyte mini, Guava Technologies). Results are expressed as % GFP transfected cells.

Cytotoxicity studies

The cytotoxicity of PEI, PEG-*b*-PEI, Man_3-PEG-*b*-PEI and Man-PEG-*b*-PEI in complexes (N/P=8) against DC2.4 cells was assessed using a modified 3-(4,5-dimethylthiazol-2-yl)-2,5-diphenyltetrazolinium bromide (MTT) assay. Briefly, cells were seeded into 96-well plates (1.5×10^5 cells/well), allowed to grow for 24 h (37°C, 5% CO_2), and then transfected with Man_3-PEG-*b*-PEI/pGFP and Man-PEG-*b*-PEI/pGFP complexes, prepared as described above. PEI/pGFP and PEG-*b*-PEI/pGFP were used as controls. Following 48 h of incubation,, the medium was discarded, and MTT solution (5 mg/ml MTT in PBS) was added into each well to a final concentration of 0.5mg/ml. Following 3 h incubation, the he medium was discarded and 200 μl of DMSO were added to dissolve formazan crystals. The absorbance of each sample was measured at 570 nm using a microplate reader (Infinite M200, TECAN, Switzerland). Cell viability is expressed as the percentage of non-transfected (control) cells.

Free mannose competition assay

THP-1, DC2.4 and HeLa cells were seeded in 96-well plates (1.5×10^5 cells/well), for 24 h at 37°C. Thirty minutes before transfection, the medium in the mannose$^+$ group was replaced with medium containing 10 mM mannose. Cells were transfected with Man_3-PEG-*b*-PEI/pGFP, Man-PEG-*b*-PEI/pGFP, PEI/pGFP and PEG-*b*-PEI/pGFP at a N/P ratio of 8. Three hours after transfection, wells were washed twice with PBS and 1 ml of fresh medium (without mannose) was added to the wells. Twenty-four hours later, the cells were collected, washed with PBS and analyzed by flow cytometry to quantify GFP positive cells, (excitation achieved at 488 nm, with emission measured at 515-535 nm).

Uptake by DCs *in vivo*

PEI/DNA, PEG-*b*-PEI/DNA, Man-PEG-*b*-PEI/DNA and Man_3-PEG-*b*-PEI/DNA at N/P=8 were prepared by dissolving the copolymers in water for injection. Further dilution was achieved by adding an equal volume of a sterile isotonic 10% glucose (w/v) solution to obtain a final concentration of 5% glucose. Plasmid GFP solution (15 μg) was added to an equal volume of copolymer solution, the mixtures were vortexed for 15 seconds and left undisturbed at room temperature for 20 min. C57/BL6 mice were injected subcutaneously at the tail base with a total volume of 80 μL. Twenty-four hours later, the mice were sacrificed the subiliac lymph nodes were removed and digested in complete RPMI media containing 500 U/mL of collagenase at 37°C for 30 min. The samples were then homogenized for 5 sec. The resulting single-cell suspension was washed with PBS containing 1% BSA and re-suspended in FACS buffer. $CD11c^+$ cells were stained with APC-labeled anti-mouse-CD11c antibody (BD Pharmingen, Franklin Lakes, NJ). Fluorescence intensity from GFP produced by the $CD11c^+$ cells was quantified by flow cytometry.

Statistical analysis

Statistical calculations were carried out using GraphPad Prism v.5 software (GraphPad Software, San Diego, CA). To identify statistically significant differences, one-way ANOVA with Bonferroni's post-test analysis was performed. Differences were considered significant if $P<0.05$(*), $P<0.01$(**) or $P<0.001$(***) and are marked accordingly in the figures.

RESULTS AND DISCUSSION

MR recognizes mannose- and fucose-terminated glycans on the surface of pathogens and plays a crucial role in antigen cross-presentation [40, 41]. Several Man-PEI conjugates formulations have been synthesized and used for MR-targeted gene delivery into antigen-presenting DCs and macrophages. While some of these studies demonstrated that Man-PEI conjugates are very effective in gene delivery via mannose receptor [30] their transfection potential was limited due to their relative toxicity at the optimal polycation/DNA ratio of 1:1 (w/w) [42]. In the present study, we designed and synthesized PEGylated PICs displaying mannosylated ligands in mono- and tri-valent-orientation to target MR-expressing DCs. The PEG shield was added to reduce the positive charge of PEI and decrease its potential toxicity. Multivalent mannosylated ligand was employed to improve the binding affinity and selectivity to DCs, which is especially important in DNA vaccination that demands highly efficient delivery of antigen-encoded DNA to specific cells.

Monovalent- and trivalent-mannosylated ligands (Man-PAP and Man_3-AHT, respectively) were synthesized as described in the Experimental section (Fig. 1) and their identity and purity was confirmed by TLC and MALTI-TOF, respectively. Man-PAP migrated with R_f = 0.57 on the TLC plate developed in ethyl acetate:isopropanol:acetone (5:3:2). MALDI-TOF analysis identified Man_3-AHT (calculated molecular weight, 720 g/mol) as molecular weight species of 743 and 759 g/mol, corresponding to M + Na and M + K adducts, respectively. Man-PAP and Man_3-AHT were then coupled to MAL-PEG-NHS, and the resulting Man-PEG-MAL or Man_3-PEG-MAL was conjugated to thiolated linear PEI to yield the final Man-PEG-*b*-PEI or Man_3-PEG-*b*-PEI block-copolymers (Fig. 2). PEG-*b*-PEI was synthesized and used as a control. ^{1}H-NMR spectra of PEG-*b*-PEI, Man-PEG-*b*-PEI and Man_3-PEG-*b*-

PEI collected in deuterated water (Fig. 3) show the characteristic shifts of PEI (δ2.8) and PEG (δ3.6) in all three block-copolymers. The estimated Man content of Man_3-PEG-*b*-PEI was there times higher than in Man-PEG-*b*-PEI, as determined by a phenol/sulfuric acid assay (Fig. 3, inset). This confirms the success of the conjugation of the Man- and Man_3-based targeting moieties to the PEG-*b*-PEI copolymer.

To test the DNA condensation ability of Man_3-PEG-*b*-PEI/DNA, Man-PEG-*b*-PEI/DNA, PEG-*b*-PEI/DNA and PEI/DNA, the quenching of ethidium bromide fluorescence was analyzed. According to the results depicted in Fig. 4, an N/P>4 was sufficient for complexation using PEI, PEG-*b*-PEI and mannosylated-PEG-*b*-PEI. Further experiments were, therefore, performed with complexes at N/P=8. In order to determine the size and surface charge of the formed PICs at N/P=8, their corresponding mean hydrodynamic size and ζ-potentials were measured. The ζ-potential of PEG-*b*-PEI/DNA, Man-PEG-*b*-PEI/DNA and Man_3-PEG-*b*-PEI/siRNA were significantly lower than that measured for PEI polyplexes (Table 1). All PICs displayed positive ζ-potentials owing to an excess of PEI over DNA. The ζ-potential of the mannosylated PEG-*b*-PEI/DNA complexes rose upon increasing the N/P ratio from 5 to 10, however, the surface charge of these complexes was significantly lower than that of PEI/DNA polyplexes (Table 1). DLS measurements were then used to determine the mean hydrodynamic size of the polyplexes (Table 1). Although PEI exhibit excellent DNA condensing properties at the N/P ratio used, the attained particles were larger than expected, being over 1000 nm in size, most probably due to aggregate formation [43].The aggregation process of PEI/DNA polyplexes in high ionic strength medium (150 mM NaCl) was reported in many previous works [39, 44]. PEGylated PEI/DNA complexes demonstrated a smaller hydrodynamic size, with a mean diameter of about 100 nm for N/P ratios of 5 and 10. The size of Man-PEG-*b*-PEI/DNA complexes grew upon

increasing the N/P ratio from 5 to 10 and was about 250 nm in size at the highest N/P ratio measured. Man_3-PEG-*b*-PEI/DNA complexes generally increased in size with augmentation of the N/P ratio (from 129 to 460 nm). The increase in the mean diameter of the mannosylated polyplexes relative to PEG-*b*-PEI/DNA could be attributed to the projection of hydrophilic mannose molecules on the exterior of the polyplexes that could cause steric interruptions and lead to a less packed particle with a larger hydrodynamic diameter. It was previously shown that the PEG chains in PEG-*b*–PEI copolymers must attain a minimum molecular weight of about 5 kDa to prevent complex aggregation [45]. In our case, using a 3.5 kDa PEG chain was sufficient to prevent aggregation. We assume that mannosylation contributes to surface shielding of the PICs to provide enhanced stability and reduced cytotoxicity.

We employed the murine dendritic cell line DC2.4 as an APC cell line model to evaluate transfection efficiency of our newly designed gene delivery system. DC2.4 cells are known to express MR [46]. Cells were transfected with Man_3-PEG-*b*-PEI, Man-PEG-*b*-PEI, PEG-*b*-PEI or PEI-encapsulated pCMVLuc or pGFP at N/P=8. Twenty-four hours after transfection, luciferase gene expression and GFP activity were tested. PEI/DNA polyplexes showed the highest gene activity *in vitro*, whereas addition of PEG significantly reduced gene activity (Fig. 5 and 6). This reduction could be attributed to the lower surface charge of the PEG-*b*-PEI/DNA complexes, as confirmed by the ζ-potential measurements, and the low adsorption to the negatively charged cell membrane. Man_3-PEG-*b*-PEI demonstrated a 3-4-fold greater transfection efficiency relative to Man-PEG-*b*-PEI in MR positive DC2.4 cells, and showed almost equal efficiency when compared to PEI/DNA. The transfection efficiency of the mannosylated PICs was significantly inhibited by free mannose in DC2.4 and THP-1 cells (Fig. 7A and B, respectively), indicating the contribution of mannose-based

targeting moieties to the increase in transfection efficiency. Of the different PICs tested, only PEI/DNA complexes were effective in transfecting HeLa cells that do not express the MR on the cell surface (Fig. 7C). Indeed, the activity of PEI/DNA complexes was not affected by the presence of free mannose, confirming the cell specificity of the mannosylated PICs. The results further demonstrate that DCs are more difficult to transfect than are HeLa cells. While ~50% of HeLa cells were transfected with PEI/DNA complexes, only ~15% of the DCs were affected by the same formulation. Still, Man_3-bearing PICs were capable of transfecting 12-15% of antigen-presenting DCs. Since only few DCs are required to initiate an immune response [2, 47], Man_3-PEG-*b*-PEI emerges as a promising gene carrier for immunotherapeutic manipulations.

During the design of the targeting ligand we hypothesized that our trivalent ligand comprises three Man molecules would allow multivalent interactions with multiple CRDs on the MR, and thus increase transfection efficiency. The transfection experiments showed that Man_3-PEG-PEI/DNA exhibited 3-fold greater transfection efficiency than did Man-PEG-PEI in MR-positive cells. Nonetheless, the maximum enhancement level was 3.8-fold for trivalent over monovalent Man, which amounts to an only 1.3-fold enhancement when corrected to a per-sugar basis. This is less remarkable than other instances of multivalent interactions that are triggered by clustering effects. Moderate enhancement in binding affinity mediated by multivalent ligand has been previously documented [34, 36]. The most acceptable explanation for this phenomenon is that the orientation of the mannose molecules in Man_3-AHT does not perfectly match the distance between the CRDs on MR. This situation would only cause an increase in the statistical chance for a mannose molecule to encounter a CRD, thus causing an additive rather than a multivalency effect.

The cytotoxicity of the different PICs was assessed by determining the growth inhibitory activity of each complex against DC2.4 cells 24 h after transfection with the various PICs together with or without pGFP (Fig. 8). The results indicated the relatively high cytotoxicity of PEI/DNA polyplexes, with only 42% of the cells being viable after treatment. This value is in agreement with previous reports in the literature [48-50]. This cytotoxicity can be attributed to the positive charge of PEI that causes non-specific adsorption to cells via electrostatic interactions with the negatively charged cell membrane. PEGylated and mannosylated PICs demonstrated reduced *in vitro* cytotoxicity when compared to the PEI building block, with 83-96% cell viability post-transfection being seen with the former pair.

In preliminary experiment, we investigated the transfection efficiency of our gene delivery systems *in vivo.* Man_3-PEG-*b*-PEI/DNA, Man-PEG-*b*-PEI/DNA, PEG-*b*-PEI/DNA or PEI/DNA polyplexes containing pGFP at N/P=8 were injected into the tail base of C57/BL6 mice. This particular site was chosen for injection because of enhanced lymphatic drainage to the inguinal lymph node in mice [51]. Twenty-four hours post-injection, the percentages of GFP positive cells in the entire cell population and in the CD11c + cells taken from the inguinal lymph nodes were measured. When examining the entire cells population extracted from the lymph node, no significant change was observed in GFP activity between the treatments. Of the different PICs, only PEI showed detectable (0.333%) GFP activity (Fig. 9A). However, Man_3-PEG-*b*-PEI/DNA and Man-PEG-*b*-PEI/DNA were 3.2- and 1.9-fold more efficient, respectively, in transfecting DCs hosted at the injection site draining lymph nodes, as compared to PEI/DNA complexes (Fig. 9B, Fig. 2s). The decrease in transfection efficiency of the PEI/DNA complexes *in vivo* as opposed to *in vitro* can be explained by the lack of cell specificity of the positively charged PEI/DNA complexes. It is possible

that the PEI/DNA complexes adhered to the cell membranes at the site of injection, thus lowering their concentration at the draining lymph nodes. This assumption needs to be further validated in future by testing tissue samples taken from the site of injection. In future experiments, we will further test whether the mannosylated PICs are taken up by APCs at the site of injection or instead migrate to the draining lymph nodes and are taken up there by APCs.

CONCLUSIONS

In this work, we have successfully synthesized an antigen-presenting DC-targeted gene delivery system composed of mannosylated-PEG conjugated to linear PEI. Man-PEG-*b*-PEI and Man_3-PEG-*b*-PEI showed good *in vitro* complexation with DNA at N/P ratios >4, had diminished surface charge, reduced hydrodynamic size and lower *in vitro* cytotoxicity than did their PEI building block. All mannosylated PICs demonstrated *in vitro* selectivity towards MR-expressing cells and superior *in vivo* CD11c+ transfection efficiency, as compared with the PEI building block. The mannosylated-PEG-*b*-PEI vehicle was shown to be a safe and efficient gene carrier to DCs, suitable for *in vivo* gene delivery. The route of injection evaluated in this work mimics an infection in the periphery, when peripheral DCs become activated and migrate to the draining lymph nodes to initiate adaptive immune responses. In future studies, we shall evaluate whether loading this system with a tumor-specific antigen encoding DNA could result in DC-targeting *in vivo* to induce an effective immune response and enhance vaccine efficiency, especially when combined with agents that elicit complementary activation signals.

ACKNOWLEDGMENTS

This work was supported by the Israeli National Nanotechnology Initiative for a Focal Technology Area (FTA) on Nanomedicines for Personalized Theranostics. We thank Mazal Rubin for her valuable assistance during this project.

REFERENCES

.1 Banchereau, J.; Steinman, R. M. Dendritic cells and the control of immunity. *Nature* **1998,** *392*, 245-52.

.2 Steinman, R. M.; Pope, M. Exploiting dendritic cells to improve vaccine efficacy. *The Journal of clinical investigation* **2002,** *109*, 1519-26.

.3 Pack, D. W.; Hoffman, A. S.; Pun, S.; Stayton, P. S. Design and development of polymers for gene delivery. *Nat Rev Drug Discov* **2005,** *4*, 581-93.

.4 De Smedt, S. C.; Demeester, J.; Hennink, W. E. Cationic polymer based gene delivery systems. *Pharm Res* **2000**113-26. ,17 ,

.5 Gao, X.; Huang, L. Cationic liposome-mediated gene transfer. *Gene therapy* **1995,** *2*, 710-22.

.6 Gebhart, C. L.; Kabanov, A. V. Evaluation of polyplexes as gene transfer agents. *Journal of controlled release : official journal of the Controlled Release Society* **2001,** *73*, 401-16.

.7 Boussif, O.; Lezoualc'h, F.; Zanta, M. A.; Mergny, M. D.; Scherman, D.; Demeneix, B.; Behr, J. P. A versatile vector for gene and oligonucleotide transfer into cells in culture and in vivo: polyethylenimine. *Proc Natl Acad Sci U S A* **1995,** *92*, 7297-301.

.8 Cho, Y. W.; Kim, J. D.; Park, K. Polycation gene delivery systems: escape from endosomes to cytosol. *J Pharm Pharmacol* **2003,** *55*, 721-34.

.9 Dash, P. R.; Read, M. L.; Barrett, L. B.; Wolfert, M. A.; Seymour, L .W. Factors affecting blood clearance and in vivo distribution of polyelectrolyte complexes for gene delivery. *Gene therapy* **1999,** *6*, 643-50.

.10 Plank, C.; Mechtler, K.; Szoka, F. C., Jr.; Wagner, E. Activation of the complement system by synthetic DNA complexes: a potential barrier for intravenous gene delivery. *Hum Gene Ther* **1996,** *7*, 1437-46.

.11 Ward, C. M.; Read, M. L.; Seymour, L. W. Systemic circulation of poly(L-lysine)/DNA vectors is influenced by polycation molecular weight and type of DNA: differential circulation in mice and rats and the implications for human gene therapy. *Blood* **2001,** *97*, 2221-9.

.12 Kabanov, A. V.; Vinogradov, S. V.; Suzdaltseva, Y. G.; Alakhov, V. Water-soluble block polycations as carriers for oligonucleotide delivery .*Bioconjugate chemistry* **1995,** *6*, 639-43.

.13 Wolfert, M. A.; Schacht, E. H.; Toncheva, V.; Ulbrich, K.; Nazarova, O.; Seymour, L. W. Characterization of vectors for gene therapy formed by self-assembly of DNA with synthetic block co-polymers. *Hum Gene Ther* **1996,** *7*, 2123-33.

.14 Katayose, S.; Kataoka, K. Water-soluble polyion complex associates of DNA and poly(ethylene glycol)-poly(L-lysine) block copolymer. *Bioconjugate chemistry* **1997,** *8*, 702-7.

.15 Petersen, H.; Fechner, P. M.; Martin, A. L.; Kunath, K ;.Stolnik, S.; Roberts, C. J.; Fischer, D.; Davies, M. C.; Kissel, T. Polyethylenimine-graft-poly(ethylene glycol) copolymers: influence of copolymer block structure on DNA complexation and biological activities as gene delivery system. *Bioconjugate chemistry* **2002,** *13*, 845-54.

.16 Bergstresser, P. R.; Fletcher, C. R.; Streilein, J. W. Surface densities of Langerhans cells in relation to rodent epidermal sites with special immunologic properties. *The Journal of investigative dermatology* **1980,** *74*, 77-80.

.17 Cella, M.; Sallusto, F.; Lanzavecchia, A. Origin, maturation and antigen presenting function of dendritic cells. *Current opinion in immunology* **1997,** *9*, 10-6.

.18 Katz, S. I.; Cooper, K. D.; Iijima, M.; Tsuchida, T. The role of Langerhans cells in antigen presentation. *The Journal of investigative dermatology* **1985,** *85*, 96s-98s.

.19 Nunez, R. Revision of the functional analysis and structural features of immortalized dendritic cell lines derived from mice lacking both type I and type II interferon receptors. *Immunology letters* **1999,** *68*, 173-86.

.20 McKenzie, E. J.; Taylor, P. R.; Stillion, R. J.; Lucas, A. D.; Harris, J.; Gordon, S.; Martinez-Pomares, L. Mannose receptor expression and function define a new population of murine dendritic cells. *Journal of immunology* **2007,** *178*, 4975-83.

.21 Stahl, P. D. The mannose receptor and other macrophage lectins. *Current opinion in immunology* **1992,** *4*, 49-52.

.22 Taylor, P. R.; Martinez-Pomares, L.; Stacey, M.; Lin, H. H.; Brown, G. D.; Gordon, S. Macrophage receptors and immune recognition. *Annu Rev Immunol* **2005,** *23*, 901-44.

.23 Apostolopoulos, V.; Barnes, N.; Pietersz, G. A.; McKenzie, I. F. Ex vivo targeting of the macrophage mannose receptor generates anti-tumor CTL responses. *Vaccine* **2000,** *18*, 3174-84.

.24 Hattori, Y.; Kawakami, S.; Lu, Y.; Nakamura, K.; Yamashita, F.; Hashida, M. Enhanced DNA vaccine potency by mannosylated lipoplex after intraperitoneal administration. *J Gene Med* **2006,** *8*, 824-34.

.25 Hu, Y.; Xu, B.; Ji, Q.; Shou, D.; Sun, X.; Xu, J ;.Gao, J.; Liang, W. A mannosylated cell-penetrating peptide-graft-polyethylenimine as a gene delivery vector. *Biomaterials* **2014,** *35*, 4236-46.

.26 Jiang, H. L.; Kim, Y. K.; Arote, R.; Jere, D.; Quan, J. S.; Yu, J. H.; Choi, Y. J.; Nah, J. W.; Cho, M. H ;.Cho, C. S. Mannosylated chitosan-graft-polyethylenimine as a gene carrier for Raw 264.7 cell targeting. *Int J Pharm* **2009,** *375*, 133-9.

.27 Kim, N.; Jiang, D.; Jacobi, A. M.; Lennox, K. A.; Rose, S. D.; Behlke, M. A.; Salem, A. K. Synthesis and characterization of mannosylated pegylated polyethylenimine as a carrier for siRNA. *Int J Pharm* **2012,** *427*, 123-33.

.28 Lu, Y.; Kawakami, S.; Yamashita, F.; Hashida, M. Development of an antigen-presenting cell-targeted DNA vaccine against melanoma by mannosylated liposomes. *Biomaterials* **2007,** *28*, 3255-62.

.29 Sun, X.; Chen, S.; Han, J.; Zhang, Z. Mannosylated biodegradable polyethyleneimine for targeted DNA delivery to dendritic cells. *International journal of nanomedicine* **2012,** *7*, 2929-42.

.30 Diebold, S. S.; Plank, C.; Cotten, M.; Wagner, E.; Zenke, M. Mannose receptor-mediated gene delivery into antigen presenting dendritic cells. *Somatic cell and molecular genetics* **2002,** *27*, 65-74.

.31 Kawakami, S.; Sato, A.; Nishikawa, M.; Yamashita, F.; Hashida, M. Mannose receptor-mediated gene transfer into macrophages using novel mannosylated cationic liposomes. *Gene therapy* **2000,** *7*, 292-9.

.32 Li, M.; Jiang, Y.; Xu, C.; Zhang, Z.; Sun, X. Enhanced immune response against HIV-1 induced by a heterologous DNA prime-adenovirus boost vaccination using

mannosylated polyethyleneimine as DNA vaccine adjuvant. *International journal of nanomedicine* **2013,** *8*, 1843-54.

.33 Biessen, E. A.; Noorman, F.; van Teijlingen, M. E.; Kuiper, J.; Barrett-Bergshoeff, M.; Bijsterbosch, M. K ;.Rijken, D. C.; van Berkel, T. J. Lysine-based cluster mannosides that inhibit ligand binding to the human mannose receptor at nanomolar concentration. *J Biol Chem* **1996,** *271*, 28024-30.

.34 Espuelas, S.; Thumann, C.; Heurtault, B.; Schuber, F.; Frisch, B .Influence of ligand valency on the targeting of immature human dendritic cells by mannosylated liposomes. *Bioconjugate chemistry* **2008,** *19*, 2385-93.

.35 Berges, C.; Naujokat, C.; Tinapp, S.; Wieczorek, H.; Hoh, A.; Sadeghi, M.; Opelz, G.; Daniel, V. A cell line model for the differentiation of human dendritic cells. *Biochem Biophys Res Commun* **2005,** *333*, 896-907.

.36 David, A.; Kopeckova, P.; Rubinstein, A.; Kopecek, J. Enhanced biorecognition and internalization of HPMA copolymers containing multiple or multivalent carbohydrate side-chains by human hepatocarcinoma cells. *Bioconjugate chemistry* **2001,** *12*, 890-9.

.37 Hermanson, G. T., *Bioconjugate techniques* Second edition ed.; Elsevier Inc: San Diego, 2008.

.38 Saha, S. K.; Brewer, C. F. Determination of the concentrations of oligosaccharides, complex type carbohydrates, and glycoproteins using the phenol-sulfuric acid method. *Carbohydr Res* **1994,** *254*, 157-67.

.39 Kleemann, E.; Neu, M.; Jekel, N.; Fink, L.; Schmehl, T.; Gessler, T.; Seeger, W.; Kissel, T . Nano-carriers for DNA delivery to the lung based upon a TAT-derived peptide covalently coupled to PEG-PEI. *Journal of controlled release : official journal of the Controlled Release Society* **2005,** *109*, 299-316.

.40 Burgdorf, S.; Kautz, A.; Bohnert, V ;.Knolle, P. A.; Kurts, C. Distinct pathways of antigen uptake and intracellular routing in CD4 and CD8 T cell activation. *Science* **2007,** *316*, 612-6.

.41 Adams, E. W.; Ratner, D. M.; Seeberger, P. H.; Hacohen, N. Carbohydrate-mediated targeting of antigen to dendritic cells leads to enhanced presentation of antigen to T cells. *Chembiochem : a European journal of chemical biology* **2008,** *9*, 294-303.

.42 Diebold, S. S.; Kursa, M.; Wagner, E.; Cotten, M.; Zenke, M. Mannose polyethylenimine conjugates for targeted DNA delivery into dendritic cells. *J Biol Chem* **1999,** *274*, 19087-94.

.43 Sharma, V. K.; Thomas, M.; Klibanov, A. M. Mechanistic studies on aggregation of polyethylenimine-DNA complexes and its prevention. *Biotechnol Bioeng* **2005,** *90*, 614-20.

.44 Trubetskoy, V. S.; Loomis, A.; Slattum, P. M.; Hagstrom, J. E.; Budker, V. G.; Wolff, J. A. Caged DNA does not aggregate in high ionic strength solutions. *Bioconjugate chemistry* **1999,** *10*, 624-8.

.45 Petersen, H.; Merdan, T.; Kunath, K.; Fischer, D.; Kissel, T .Poly(ethylenimine-co-L-lactamide-co-succinamide): a biodegradable polyethylenimine derivative with an advantageous pH-dependent hydrolytic degradation for gene delivery. *Bioconjugate chemistry* **2002,** *13*, 812-21.

.46 Cui, Z.; Han, S. J.; Huang, L. Coating of mannan on LPD particles containing HPV E7 peptide significantly enhances immunity against HPV-positive tumor. *Pharm Res* **2004,** *21*, 1018-25.

.47 Philip, R.; Brunette, E.; Ashton, J.; Alters, S.; Gadea, J.; Sorich, M.; Yau, J.; O'Donoghue, G.; Lebkowski ,J.; Okarma, T.; Philip, M. Transgene expression in dendritic cells to induce antigen-specific cytotoxic T cells in healthy donors. *Cancer gene therapy* **1998,** *5*, 236-46.

.48 Kafil, V.; Omidi, Y. Cytotoxic impacts of linear and branched polyethylenimine nanostructures in a431 cells. *Bioimpacts* **2011,** *1*, 23-30.

.49 Florea, B. I.; Meaney, C.; Junginger, H. E.; Borchard, G. Transfection efficiency and toxicity of polyethylenimine in differentiated Calu-3 and nondifferentiated COS-1 cell cultures. *AAPS PharmSci* **2002,** *4*, E12.

.50 Lin, C. W.; Jan, M. S.; Kuo, J. H.; Hsu, L. J.; Lin, Y. S. Protective role of autophagy in branched polyethylenimine (25K)- and poly(L-lysine) (30-70K)-induced cell death. *Eur J Pharm Sci* **2012,** *47*, 865-74.

.51 Harrell, M. I.; Iritani, B. M.; Ruddell, A. Lymph node mapping in the mouse. *Journal of immunological methods* **2008,** *332*, 170-4.

Tables and Figures:

Table 1: PIC mean diameter (nm) and surface charge (mV) at different N/P ratios

Polyplex	ζ-potential (mV)		Particle size (nm)	
	N/P=5	**N/P=10**	**N/P=5**	**N/P=10**
PEI/DNA	27.8 ± 1.2	31.0 ± 4.5	>1000	>1000
PEG-*b*-PEI/DNA	NA	18.7 ± 2.3	80	111
Man-PEG-*b*-PEI/DNA	16.5 ± 0.5	20.7 ± 3.5	128	253
Man_3-PEG-*b*-PEI/DNA	12.5 ± 1	16.4 ± 4.5	129	460

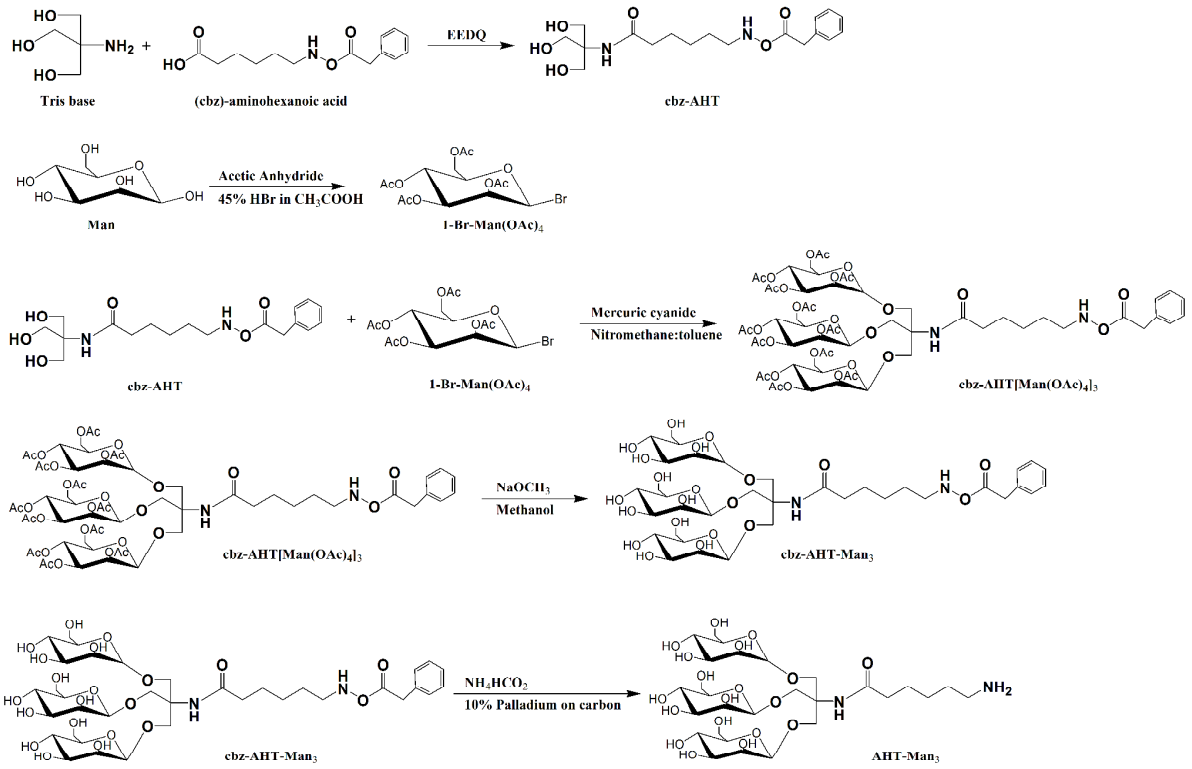

Figure 1: Reaction scheme for the synthesis of Man_3-(amidohexanamido)-Tris, Man_3-AHT. (**A**). Cbz-AHT was synthesized by coupling Tris base with Cbz-aminohexanoic acid in absolute ethanol in the presence of EEDQ. (**B**). α-D-Man was transformed 1-Br-$Man(OAc)_4$ using 45% (w/v) HBr in glacial acetic acid. (**C**). Cbz-AHT was coupled with 1-Br- $Man(OAc)_4$ in a mixture of nitromethane:toluene (1:1) in the presence of mercuric cyanide to give Cbz-AHT-$[Man(OAc)_4]_3$ conjugate. Man_3-AHT was obtained after the removal of the Cbz protecting group by hydrogenation in methanol using 10% palladium on carbon (Pd/C) in the presence of ammonium formate (NH_4HCO_2).

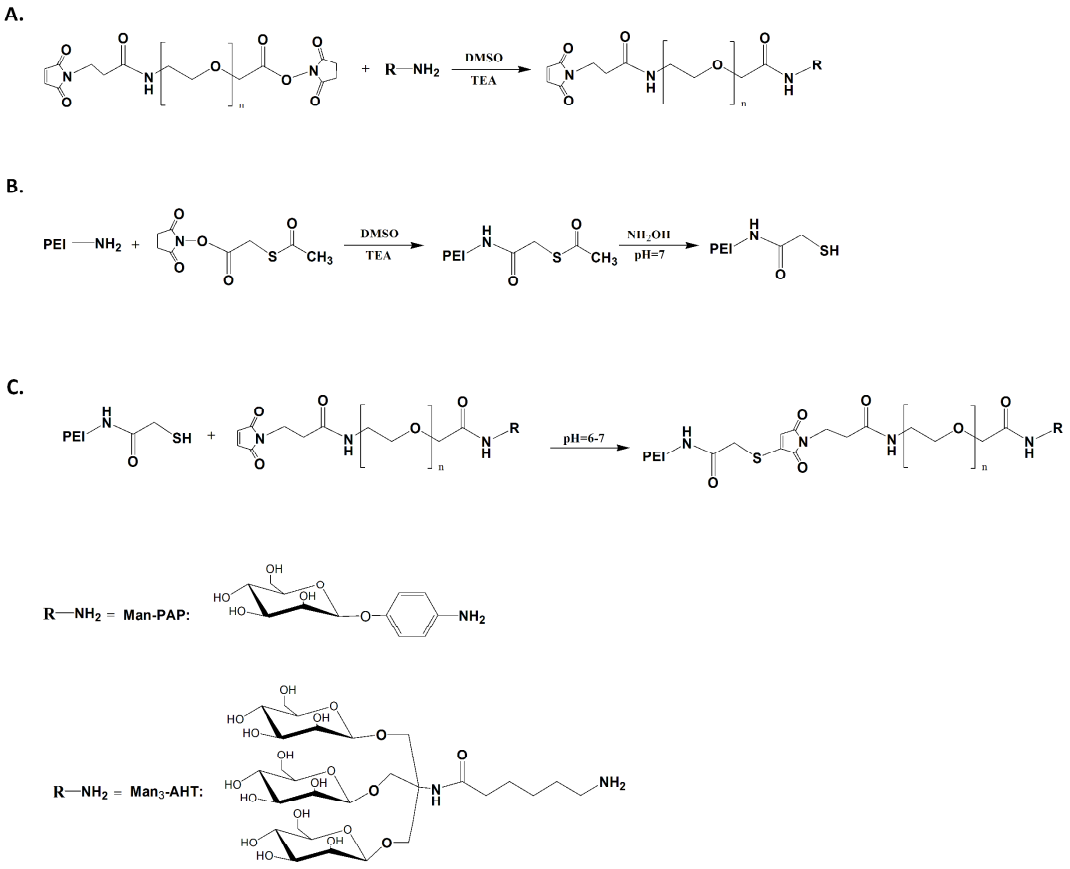

Figure 2: Three-step synthesis of Man-PEG-*b*-PEI and Man_3-PEG-*b*-PEI. (**A**). Man_3-AHT or Man-PAP was conjugated to NHS-PEG-MAL via the NHS-activated terminal in DMSO in the presence of TEA to give Man_3-PEG-MAL or Man-PEG-MAL MAL-PEG-NHS, respectively. (**B**). PEI was conjugated with SATA in DMSO in the presence of TEA and subsequently treated with NH_2OH to give PEI with free sulphydryl group. (**C**). Thiolated PEI was then conjugated to the mannosylated-PEG via the MAL-activated terminal PEI to yield the final products, Man-PEG-*b*-PEI or Man_3-PEG-*b*-PEI.

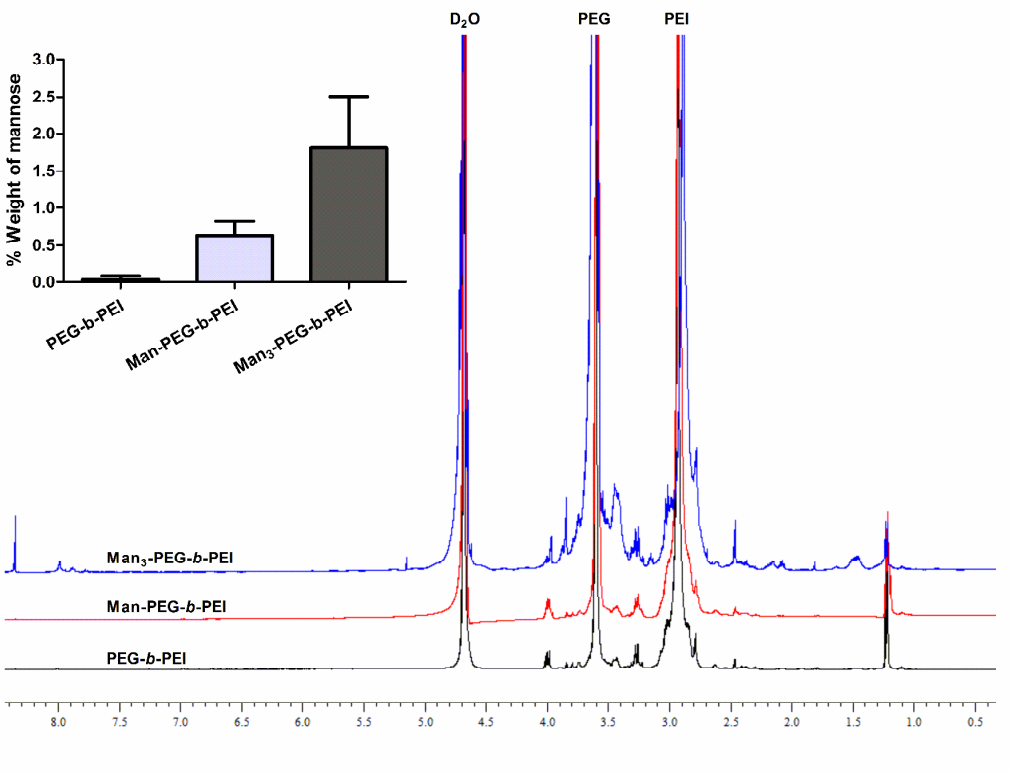

Figure 3: H^1-NMR spectra of (A) PEG-*b*-PEI, (B) Man-PEG-*b*-PEI and (C) Man_3-PEG-*b*-PEI in D_2O indicating the chemical shifts of PEG δ3.6 (s, CH_2-CH_2) and PEI δ2.8 (s, CH_2-CH_2). **Inset:** % weight of mannose in PEG-*b*-PEI, Man-PEG-*b*-PEI and Man_3-PEG-*b*-PEI conjugates calculated by a phenol/sulfuric acid assay. The results are given as means ± SD of three independent experiments.

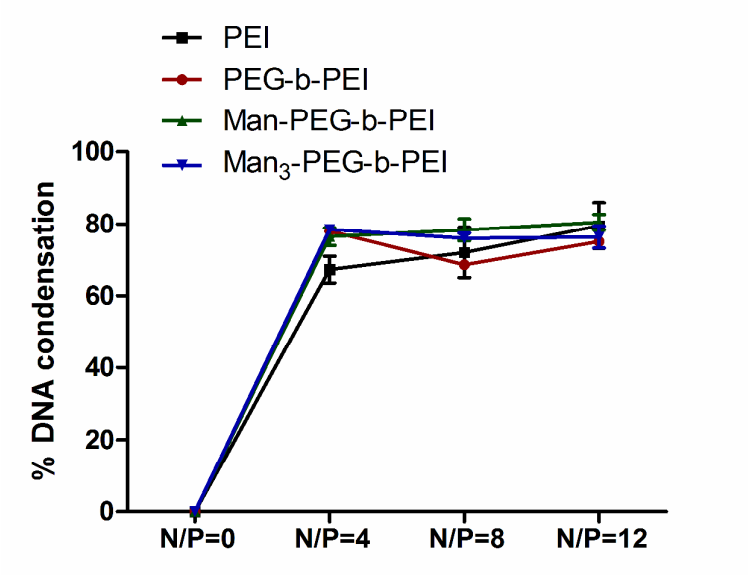

Figure 4: DNA condensation ability of PEI, PEG-*b*-PEI, Man-PEG-*b*-PEI and Man_3-PEG-*b*-PEI complexes formed with pCMVLuc at different N/P ratios in a 150 mM NaCl solution. Condensation ability was analyzed by the ethidium bromide fluorescence quenching assay. Results are given as means ± SD of three independent experiments.

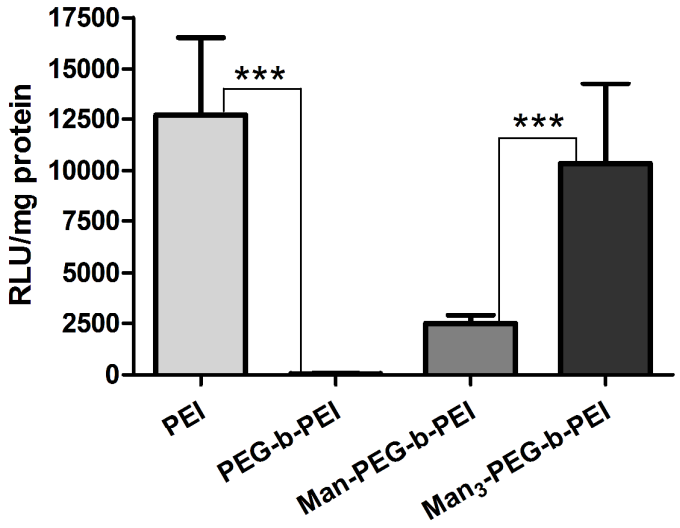

Figure 5: Transfection efficiency of the different PICs measured by luciferase activity in DC2.4 cells after a 24 h incubation with PEI/pCMVLuc, PEG-*b*-PEI/pCMVLuc, Man-PEG-*b*-PEI/pCMVLuc or Man_3-PEG-*b*-PEI/pCMVLuc at N/P=8. Relative luminescent units (RLU) were measured using a Plate Luminol Analyzer. Results are given as means ± SD of three independent experiments, ***$p<0.001$.

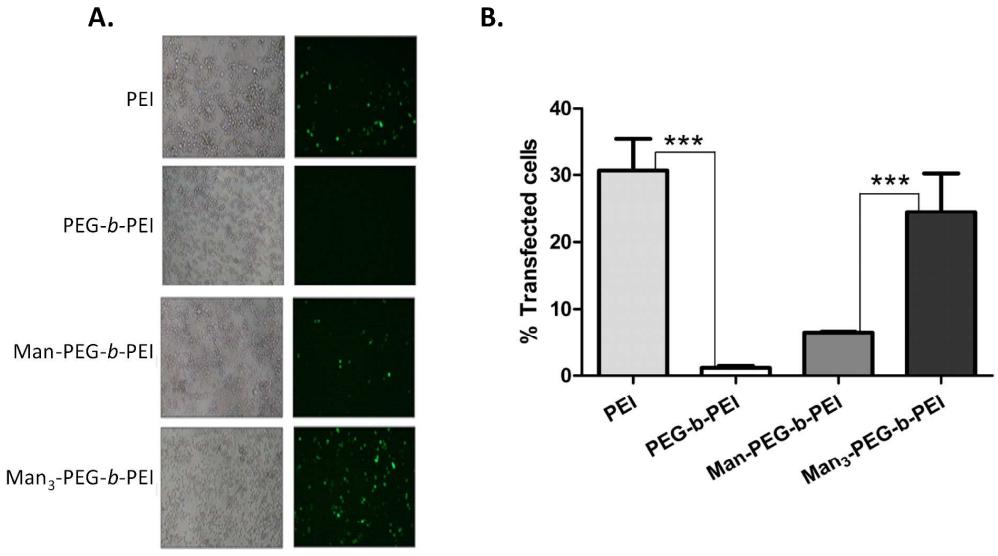

Figure 6: (A) Transfection efficiency of the different PICs visualized by GFP fluorescence in DC2.4 cells after a 24 h incubation with PEI/ pGFP, PEG-*b*-PEI/ pGFP, Man-PEG-*b*-PEI/pGFP or Man_3-PEG-*b*-PEI/pGFP at N/P=8. Pictures were taken by a fluorescence microscope. (B) Percentage of transfected DC2.4 cells after a 24 h incubation with PEI/pGFP, PEG-*b*-PEI/pGFP, Man-PEG-*b*-PEI/pGFP or Man_3-PEG-*b*-PEI/pGFP at N/P=8 measured by flow cytometry. Results are given as mean ± SD of four independent experiments, ***$p<0.001$.

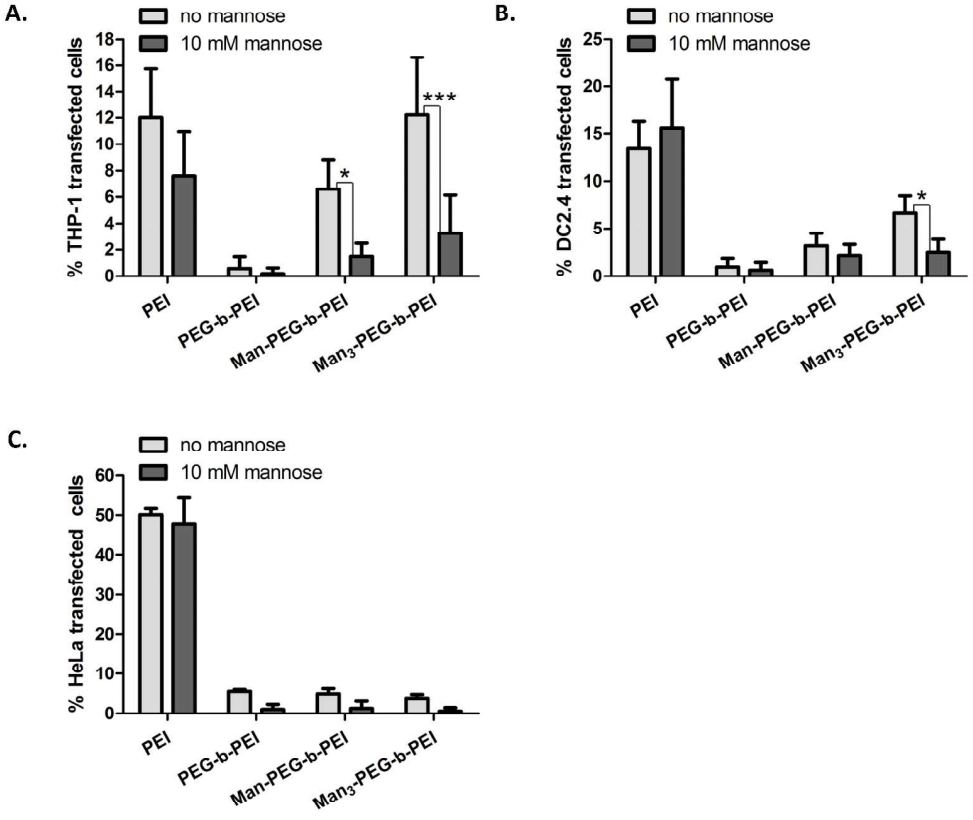

Figure 7: Transfection efficiency in THP-1 (A), DC2.4 (B), and HeLa (C) cells after a 24 h incubation with PEI/pGFP, PEG-*b*-PEI/pGFP, Man-PEG-*b*-PEI/pGFP or Man_3-PEG-*b*-PEI/pGFP at N/P=8. Polyplexes were incubated in the presence or absence of 10 mM mannose. Fluorescence was measured by flow cytometry. Results are given as mean ± SD of four independent experiments, *$p<0.05$, ***$p<0.001$.

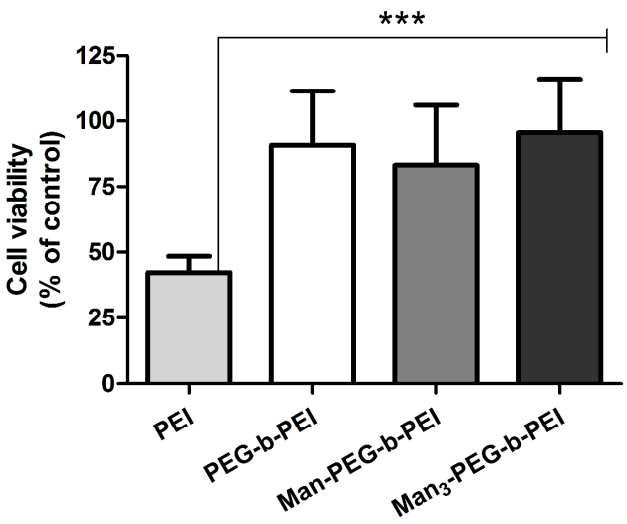

Figure 8: DC2.4 cells viability after a 24 h incubation with PEI/pGFP, PEG-*b*-PEI/pGFP, Man-PEG-*b*-PEI/pGFP or Man_3-PEG-*b*-PEI/pGFP at N/P=8. Cell viability was determined by the MTT assay, relative to non-treated cells. Results are given as mean ± SD of four independent experiments, ***$p<0.001$.

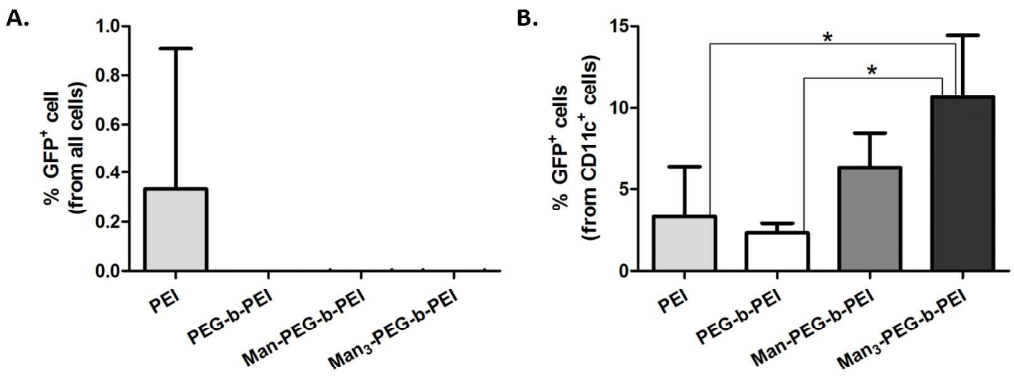

Figure 9: *In vivo* uptake of polyplexes by DCs in the draining lymph nodes of mice 24 h after subcutaneous injection. Complexes were prepared with PEI/pGFP, PEG-*b*-PEI/pGFP, Man-PEG-*b*-PEI/pGFP or Man_3-PEG-*b*-PEI/pGFP at N/P=8. Results represent the percentage of GFP^+ cells in the entire cell population (A) and in the $CD11c^+$ cell population (B), and are given as mean ± SD of three independent experiments, *$p<0.05$.

Supplemental Data

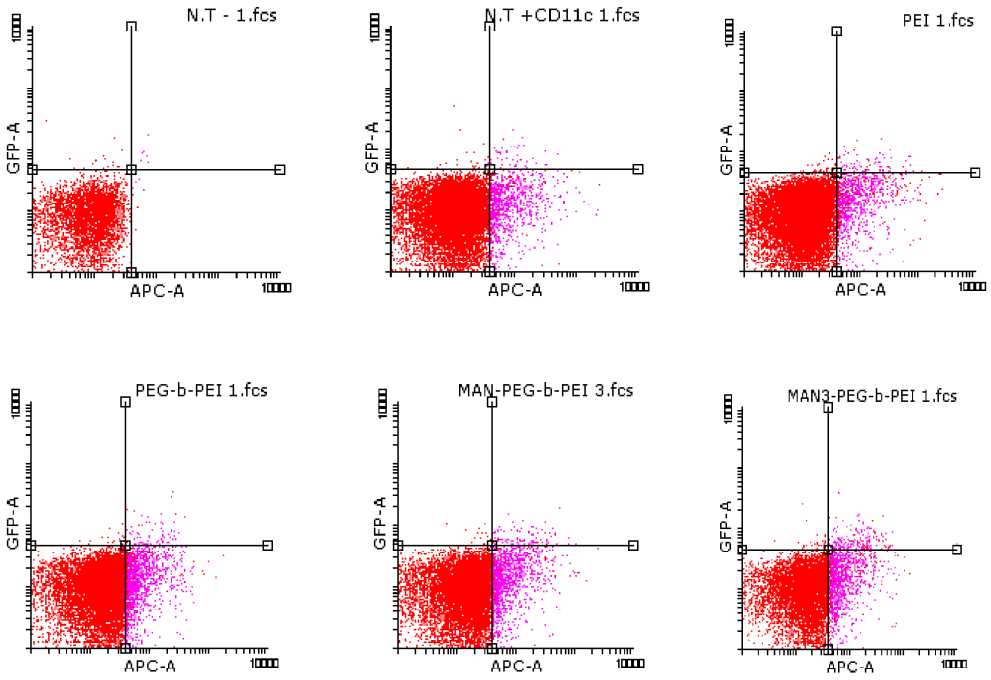

Treatment	% GFP+ cells in CD11c+ cell population
PEI/pGFP	3.51
PEG-*b*-PEI/pGFP	2.16
Man-PEG-*b*-PEI/pGFP	6.26
Man_3-PEG-*b*-PEI/pGFP	10.53

Fig. 1s: Representative flow cytometry analysis of cells taken from the inguinal lymph nodes 24 h after treatment with PEG-*b*-PEI/pGFP, PEI/pGFP, Man-PEG-*b*-PEI/pGFP and Man_3-PEG-*b*-PEI/pGFP at N/P=8. $CD11c^+$ cells were stained with APC-labeled anti-mouse-CD11c antibody. Fluorescence intensity from GFP produced by the $CD11c^+$ cells was quantified. The top right quadrant represents cells stained by both CD11c antibody and expressing GFP.

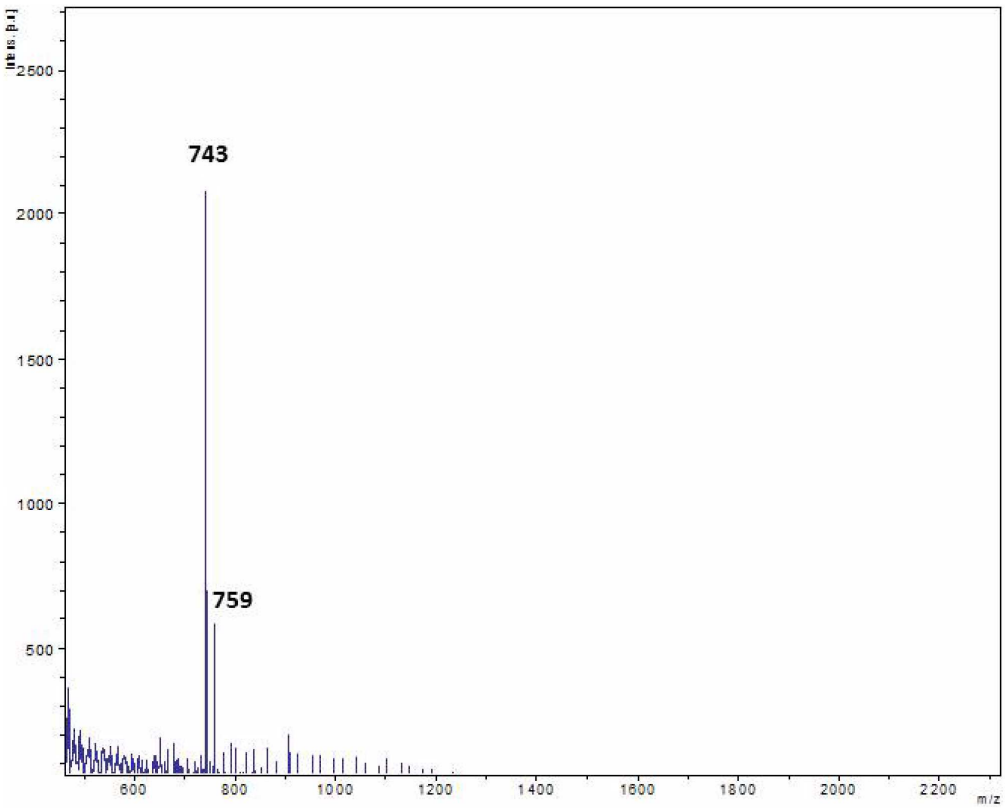

Fig. 2s: MALDI-TOF mass spectrum of Man_3-AHT (calculated Mw, 720 g/mol) showing two peaks (m/z 743 and 759) corresponding to M + Na and M + K, respectively.